JOC The Journal of Organic Chemistry

Article

pubs.acs.org/joc

Pyrene-Fluorene Hybrids Containing Acetylene Linkage as Color-Tunable Emitting Materials for Organic Light-Emitting Diodes

K. R. Justin Thomas,*[,†] Neha Kapoor,[†] M. N. K. Prasad Bolisetty,[†] Jwo-Huei Jou,[‡] Yu-Lin Chen,[‡] and Yung-Cheng Jou[‡]

[†]Organic Materials Laboratory, Department of Chemistry, Indian Institute of Technology Roorkee, Roorkee 247 667, India

[‡]Department of Material Science and Engineering, National Tsing Hua University, Hsinchu 30013, Taiwan

Supporting Information

ABSTRACT: New blue- to yellow-emitting materials have been developed by incorporating fluorene-based chromophores on pyrene core with acetylene linkage and using multifold palladium-catalyzed cross-coupling reactions. Both mono- and tetrasubstituted derivatives have been synthesized and characterized. The tetrasubstituted derivatives displayed red-shifted emission when compared to the monosubstituted derivative indicative of an extended conjugation in the former. End-capping with a diphenylamine unit further red-shifted the absorption and emission profiles and imparted a weak dipolar character to the molecules. Amine-containing derivatives displayed positive solvatochromism in the fluorescence spectra indicating a more polar excited state due to an efficient charge migration from the diphenylamine donor to the pyrene π-acceptor. All of the derivatives were tested as emitting dopants with host material 4,4′-bis(9*H*-carbazol-9-yl)biphenyl (CBP) in a multilayered OLED and found to exhibit bright blue or yellow electroluminescence. The device utilizing 1,3,6,8-tetrasubstituted pyrene derivative as a dopant emitter displayed highest maximum luminescence 4630 cd/m^2 with power efficiency 3.8 lm/W and current efficiency 7.1 cd/A at 100 cd/m^2 attributable to the proper alignment of energy levels that led to the efficient harvesting of excitons. All of the devices exhibited color purity over a wide range of operating voltages.

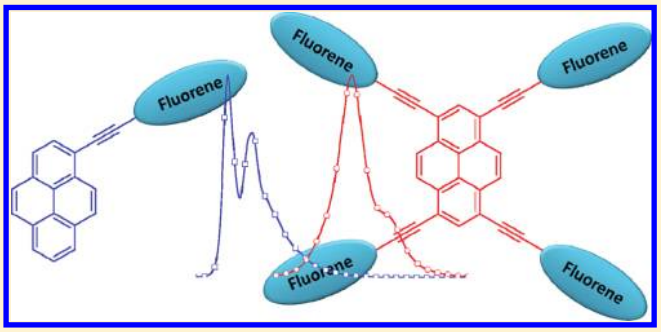

INTRODUCTION

Organic materials possessing extended π-conjugation have received immense attention in recent years owing to their unique photophysical and charge transport properties, which make them potential materials for application in electronic devices such as organic light-emitting diodes (OLEDs),[1] organic photovoltaics (OPV),[2] organic thin film transistors (OTFT),[3] etc. They are also attractive due to their promising two photon absorption[4] and nonlinear optical[5] characteristics. Among the π-conjugated molecular materials, those containing polyaromatic hydrocarbons (PAH) such as fluorene,[6] anthracene,[7] perylene,[8] pyrene,[9] pentacene,[10] carbazole,[11] etc. tethered with one another by vinyl or acetylene linkages are attractive due to their flat π-stacking organization in the solid state. Direct C−C linkage between the PAH has been found to be detrimental for the extension of conjugation as there is a loss of coplanarity due to the steric congestion.[12] However, introduction of vinyl or acetylene units as spacers between the PAH units helped the compounds to acquire planarity, which is required for efficient intramolecular and intermolecular interactions and charge transport properties.[13]

Pyrene-[14] and fluorene-based[15] functional materials have been extensively explored as active ingredients for electronic devices. Fluorene and pyrene derivatives generally displayed promising optical and electrochemical properties. The advantage associated with pyrene is the facile substitution at the 1, 3, 6, and 8 positions. Similarly, fluorene is flexible toward chemical modifications at the 2, 7, and 9 positions. It is expected that the integration of fluorene and pyrene in a molecular structure may impart favorable optical and charge transport properties desired for electronic applications. Fluorene-pyrene hybrids[16] based on 1,3,6,8-tetrasubstituted pyrene or 2,7-disubstituted fluorene[16] have been found to emit intense blue light in OLEDs. Oligomers and dendrimers featuring pyrene, fluorene, and carbazole units and acetylene linkages have been reported by Zhao et al.[17] Tetrasubstituted cruciform pyrenes have been developed and found to be useful in liquid crystals and field effect transistors.[18] Tetrasubstituted pyrene derivatives with phenyl conjugation and/or acetylene linkers were also demonstrated as blue emitters in OLEDs, two-photon absorbers, and materials exhibiting unique charge transfer dynamics due their X-shaped architecture.[19] X-shaped 1,2,4,5-tetravinyl-benzenes,[20] 1,4-bis(arylethynyl)-2,5-distyrylbenzenes,[21] and 1,2,4,5-tetrasubstituted(phenylethynyl)benzenes[22] have been extensively studied and found to exhibit interesting photophysical properties. Pyrene cored X-shaped molecules containing ethynylfluorene π-linkers have been reported as

Received: February 10, 2012
Published: March 23, 2012

Chart 1. Structures of Pyrene-Fluorene Hybrids (4−9) Containing Acetylene Bridges

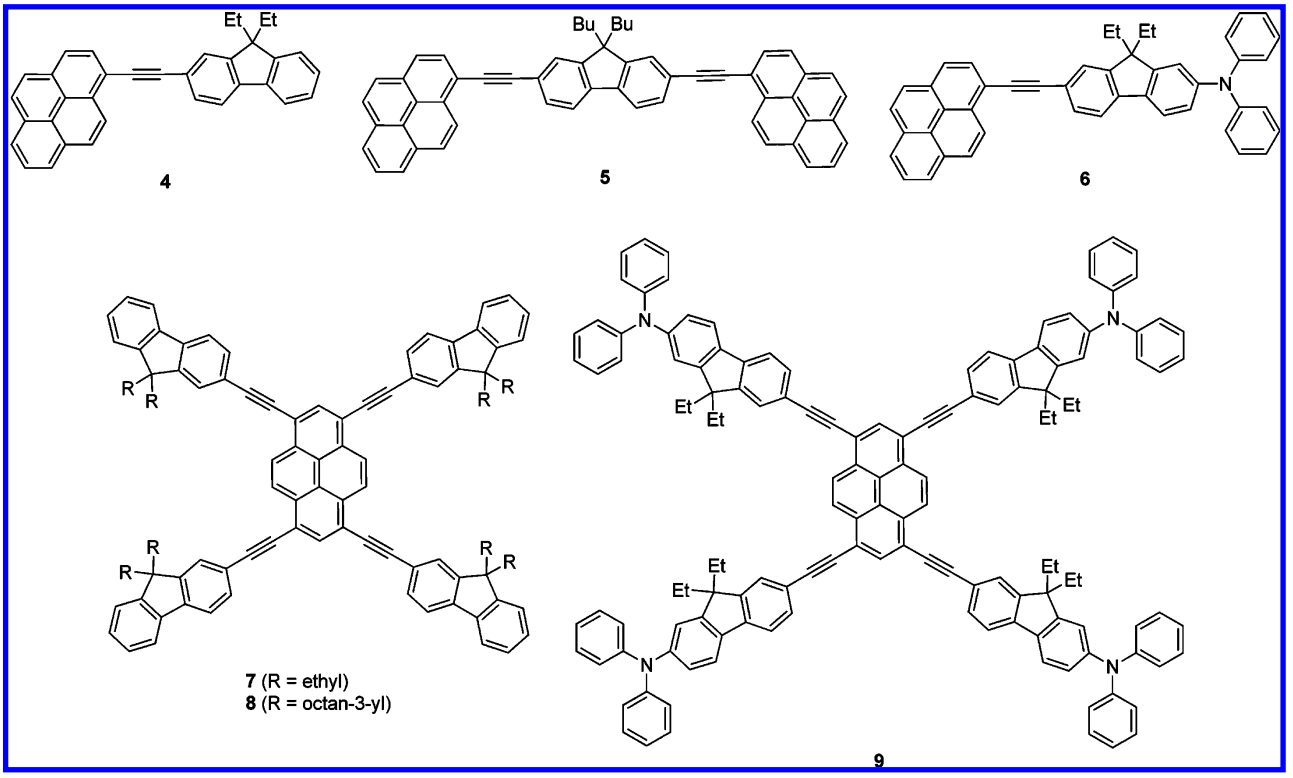

Scheme 1. Synthetic Pathway Used for the Preparation of the Compounds 4−9

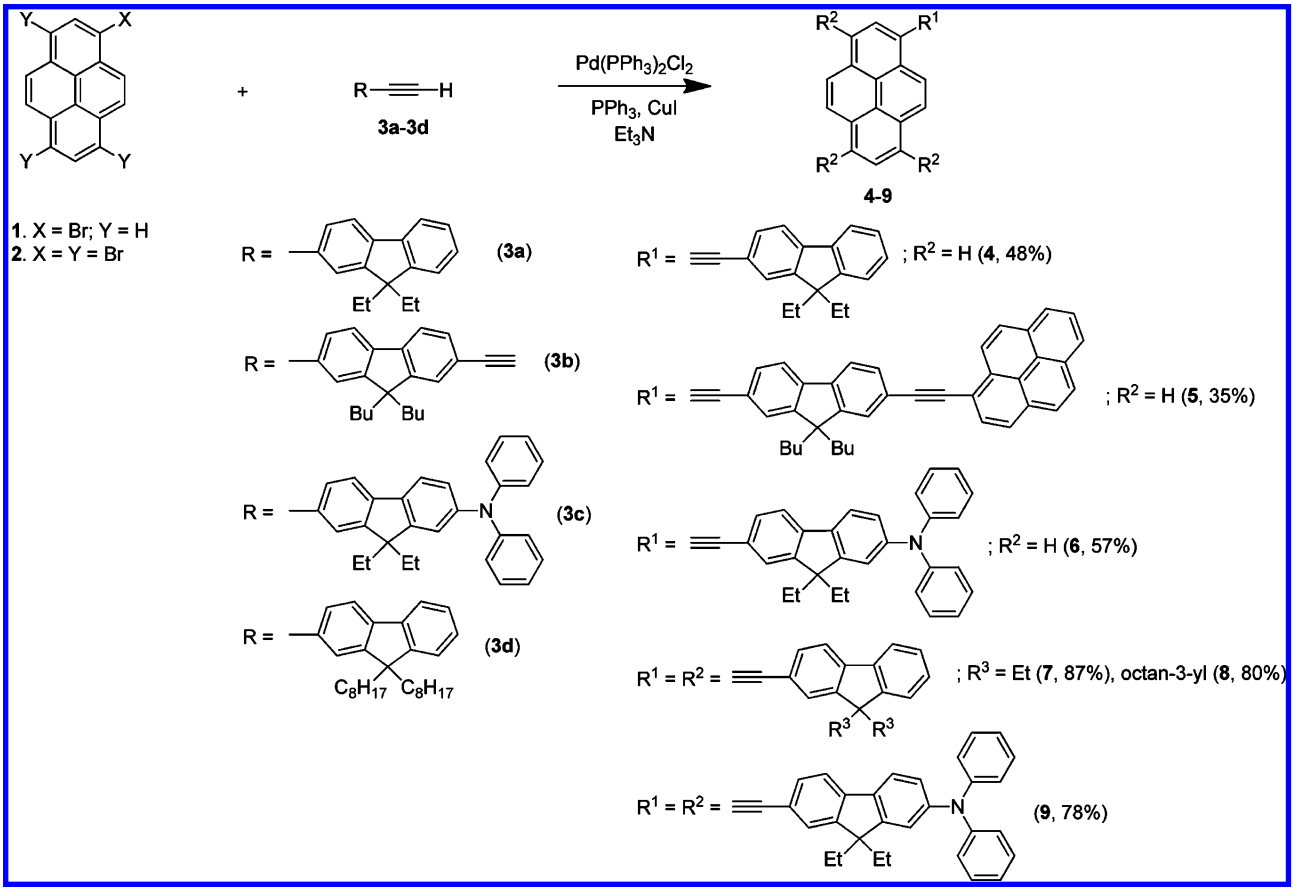

active constituents for the visual detection of heparin,[23] and the molecules that possessed carbazole end groups displayed gigantic two-photon absorption cross sections.[24] However, no systematic optical, electrochemical, theoretical, and electro-

dx.doi.org/10.1021/jo300285v | J. Org. Chem. 2012, 77, 3921−3932

luminescence investigations have been attempted on pyrene-based materials with ethynylfluorene peripheries.

In this report, we present the synthesis and photophysical and electroluminescent characteristics of the new molecular materials (Chart 1) based on a pyrene core that is connected to fluorene chromophores by acetylene units. The optical properties of the materials are highly dependent on the number of chromophores present on the pyrene nucleus. The monosubstituted derivatives display bright blue emission, while the tetrasubstituted pyrene derivatives exhibit greenish yellow emission. Compounds (**6** and **9**) containing triarylamine-terminated arms displayed red-shifted emission when compared to the corresponding parent hydrocarbons (**4** and **8**) in solution, indicative of an auxochromic effect by the amine unit. Interestingly, the amine end-capped derivatives **6** and **9** exhibited solvatochromism in the fluorescence suggestive of photoinduced intramolecular charge transfer from the amine peripheries to the pyrene core (vide supra).

RESULT AND DISCUSSION

Synthesis. The structures of pyrene-based functional materials (**4**–**9**) developed in this work are depicted in Chart 1. The synthetic route employed for preparing them is shown in Scheme 1. The synthesis was conveniently accomplished by a cross-coupling reaction (Sonogashira reaction) of 1-bromopyrene (**1**) or 1,3,6,8-tetrabromopyrene (**2**) with 9,9-diethyl-2-ethynyl-9*H*-fluorene (**3a**), 9,9-dibutyl-2,7-diethynyl-9*H*-fluorene (**3b**), 9,9-diethyl-7-ethynyl-*N*,*N*-diphenyl-9*H*-fluoren-2-amine (**3c**), and 2-ethynyl-9,9-di(octan-3-yl)-9*H*-fluorene (**3d**), respectively, by employing $Pd(PPh_3)_2Cl_2/PPh_3/CuI$ catalytic system. The terminal acetylenes, such as 9,9-diethyl-2-ethynyl-9*H*-fluorene (**3a**), 9,9-dibutyl-2,7-diethynyl-9*H*-fluorene (**3b**), and 2-ethynyl-9,9-di(octan-3-yl)-9*H*-fluorene (**3d**), required for the study have been synthesized by a two-step protocol (not shown in Scheme 1) involving Sonogashira coupling of 2-methylbut-3-yn-2-ol with the corresponding aryl bromides and the base-catalyzed cleavage of the functionalized but-3-yn-2-ols obtained in the first step.[25] Compound **7** exhibited poor solubility in common organic solvents, and to overcome this problem a derivative **8**, with long alkyl chain, was also synthesized. The dyes (**4**–**9**) are intensely colored (yellow or orange) and soluble in a wide variety of solvents including toluene, dichloromethane, acetonitrile, etc. The amine derivatives (**6** and **9**) showed better solubility in polar solvents such as acetonitrile when compared to the rest (**4**, **5**, **7**, and **8**). All of the dyes were characterized by spectral methods (NMR and HRMS), and the data is consistent with the proposed structures.

Optical Properties. The absorption spectra of compounds **4**–**9**, recorded in toluene, are displayed in Figure 1, and the pertinent data are collected in Table 1. The monosubstituted derivative **4** showed the shortest wavelength absorption, while the tetrasubstituted derivative **9** possessed the longest wavelength peak. The vibronic pattern observed for the absorption spectra of **4** is similar to pyrene,[27] but the peak position is more red-shifted when compared to pyrene. Moreover, it displayed longer wavelength absorption with larger extinction coefficient when compared to 1-(phenylethynyl)pyrene reported by Yang et al.[28] The red-shift is attributed to the extension of conjugation on replacement of the phenyl group with a fluorene unit. The pyrene-fluorene-pyrene triad **5** exhibited 15 nm bathochromism and 2-fold increase in the molar extinction coefficient when compared to **4** in agreement with the above

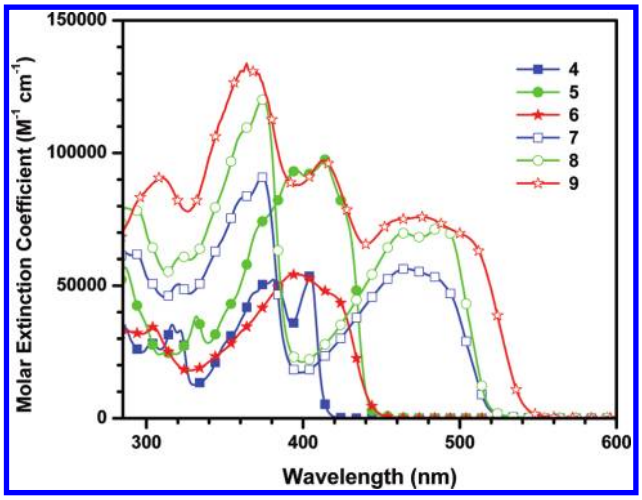

Figure 1. Absorption spectra of the dyes **4**–**9** recorded in toluene.

Table 1. Optical Data for Compounds 4–9

compound	λ_{max}, nm (ε_{max}, M^{-1} cm^{-1} × 10^3)[a]	λ_{em}, nm (Φ_F)[a,b]	Stokes' shift,[a] cm^{-1}	λ_{em} (film),[c] nm
4	286 (34.7), 304 (28.2), 316 (35.3), 322 (33.1), 381 (52.3), 405 (53.9)	412, 436 (0.99)	420	496
5	286 (56.9), 332 (38.5), 414 (97.5), 424 (82.1)	438, 463 (0.99)	754	486, 505
6	287 (33.5), 304 (34.4), 395 (54.2), 418 (46.8)	449, 475 (sh) (0.72)	1652	495
7	285, 321, 374, 466, 486	512, 548 (0.64)	1045	586
8	287(79.3), 374 (120.1), 464 (70.0), 488 (72.5)	513, 549 (0.67)	999	587
9	310 (90.8), 364 (133.8), 413 (97.2), 476 (75.9), 503 (69.0)	535, 568 (sh) (0.43)	1189	581

[a]Measured for toluene solutions. [b]Relative quantum yield was obtained by comparing with standards coumarin-1 (0.99 in ethyl acetate) or coumarin-6 (0.75 in ethanol).[26] [c]Measured for spin-cast thin film.

observation. The tetrasubstituted derivatives **7** and **8** showed two structured absorptions. The longer wavelength peak occurring at >460 nm is assigned to a π–π^* transition originating from the entire molecule, while the absorption in the 340–380 nm region may arise from the pyrene/fluorene localized π–π^* transitions (see below for theoretical interpretations). It is interesting to compare the absorption features of the compounds **7** and **8** with the known tetrasubstituted derivatives. The absorption maximum of **7** and **8** is 30 nm bathochromically shifted and displayed significantly higher molar extinction coefficient when compared to 1,3,6,8-tetrakis-(phenylethynyl)pyrene.[29] Also they exhibited a 92 nm red-shift compared to 1,3,6,8-tetrakis(9,9-dihexyl-9*H*-fluoren-2-yl)-pyrene (400 nm in THF).[30] This indicates that the incorporation of acetylene spacer between the pyrene and fluorene segments is beneficial for the absorption properties of these compounds. This may be due to the planarity achieved in the compounds **7** and **8** due to the presence of an acetylene linkage that will facilitate the extension the π-conjugation. Introduction of amine functionality further broadened the absorption profile for the compounds **6** and **9** due to the formation of new peaks attributable to the diphenylamine

dx.doi.org/10.1021/jo300285v | J. Org. Chem. 2012, 77, 3921–3932

localized transitions (<320 nm) and charge transfer transition from the amine donor to the pyrene acceptor.[31] Pyrenylamine and their derivatives have been demonstrated to display a charge transfer transition at ~400 nm.[31]

The compounds are intensely emitting in the blue to yellow region on exposure to visible light, and the corresponding emission spectra recorded for compounds **4**–**9** in toluene are displayed in Figure 2. The related data are given in Table 1. All

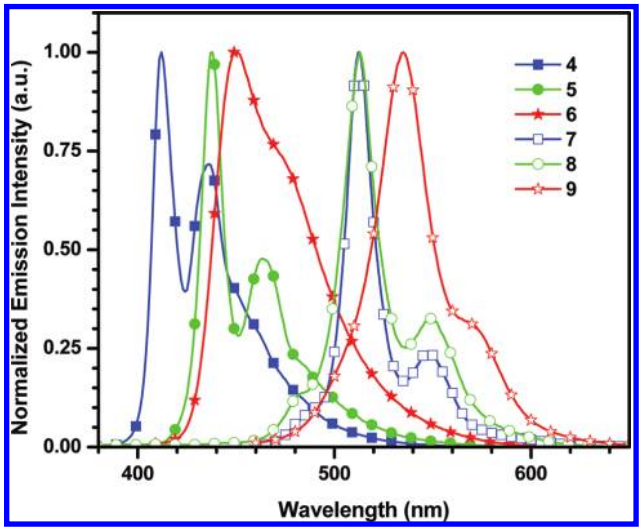

Figure 2. Emission spectra of the dyes **4**–**9** recorded in toluene.

of the compounds showed vibronic transitions in the emission spectra recorded in toluene attesting the rigidity of the structure. The emission profile of **4** is red-shifted when compared to that observed for pyrene and 1-(phenylethynyl)-pyrene (392 nm),[30] suggestive of involvement of an extended π-system in the electronic excitation. The emission wavelengths of the compounds are in the order **4** < **5** < **6** < **7** ≈ **8** < **9**. This is largely in keeping with the trend in the conjugation length present in the molecules. Though the amine-containing derivatives **6** and **9** have displayed absorption peaks similar to their parent hydrocarbons **4** and **7**, they exhibited significantly red-shifted emission peaks. This may be a result of a polarized excited state that can undergo dipolar relaxation before emission could occur.[1c,32] The larger Stokes shifts observed for the tetrasubstituted derivative (**8** and **9**) and the amine-containing compound (**6**) point to the existence of non-radiative relaxation pathways in these molecules. The fluorescence quantum yield measured by comparing with the standards indicates that these materials are promising emitters. The tetrasubstituted derivatives (**7** and **8**) and the amine-containing compounds (**6** and **9**) show relatively less quantum yield when compared to the monosubstituted analogues **4** and **5**. It is probable that the photoexcitation of above the derivatives leads to intramolecular charge transfer at the excited state (ICT). ICT normally reduces the quantum yield due to more pronounced relaxation and nonradiative decay in the excited state.[19e]

The solvatochromism study was performed for all of the dyes in different solvents to evaluate the effect of solvent polarity on the optical properties of the molecules. The absorption and emission spectra of **4**–**9** was recorded in the solvent of different polarity such as cyclohexane (CH), toluene (TOL), chloroform ($CHCl_3$), ethyl acetate (EA), tetrahydrofuran (THF), dichloromethane (DCM), *N*,*N*-dimethylformamide (DMF), and acetonitrile (ACN). The absorption and emission data observed for the dyes in selected solvents are listed in Tables 2 and 3. The derivatives **4**, **5**, and **8** showed negligible changes in absorption and emission profiles on varying the polarity of the solvent used for the measurement. However, the amine-containing derivatives **6** (Figure 3) and **9** showed prominent positive solvatochromism in the emission spectra only. This shows that the dyes **6** and **9** are more polarized in the excited state than in the ground state. It is reasonable to assume that the pyrene unit acts as a strong π-acceptor in the excited state. More polarized excited state of the molecules will be stabilized by polar solvents thus will cause a red-shift in emission.[32]

The solvatochromism data of the dyes **6** and **9** were analyzed by Lippert–Mataga plot[33] and Stokes shift versus $E_T(30)$ parameter. The dye **6** exhibited linear correlations (Figure 4) in the above-mentioned analyses, but the dye **9** showed notable deviation (Figure 5) for the data observed for dichloromethane solution from linearity in the Lippert–Mataga and $E_T(30)$ parameter correlation plots. This distortion is due to the unusual red-shift in the absorption and emission spectra observed for the dye in dichloromethane solution. Similar behavior has been earlier observed for organic dyes and attributed to the instant stabilization due to a fast rearrangement of polarizable electrons during excitation.[34]

The emission spectra were also measured for spin-cast thin films of the dyes. The peak values are presented in Table 1. Compounds **4**, **5**, and **8** exhibited red-shifted emission in thin film when compared to those observed for toluene solutions. Moreover, these derivatives showed a broad single peak in thin film without vibronic features. This clearly indicates that the red-shifted broad peak in thin film is due to molecular aggregation or excimer formation in the excited state.[35] However, the diphenylamine end-capped derivatives **6** and **9** showed no significant change in emission wavelength when recorded in thin film state. This suggests that the trigonal amine functionality effectively suppresses the formation of aggregates for **6** and **9** in the solid state.[36]

Electrochemical Characteristics. The electrochemistry of the compounds was studied by cyclic voltammetric measurements using a three electrode assembly comprising a glassy carbon working, platinum auxiliary, and nonaqueous Ag/$AgNO_3$ reference electrodes. The redox potentials were calibrated by using ferrocene as an internal standard. The data are listed in Table 4, and the cyclic voltammograms measured for the selected dyes (**6**, **8**, and **9**) are presented in Figure 6. From Table 4 and Figure 6, it can be observed that all of the compounds display an oxidation wave arising from the conjugation backbone. This oxidation is irreversible in the molecules **4** and **5** but appeared as a quasi-reversible process in the rest of the dyes (**6**, **8**, and **9**). The electron-richness in these molecules is significantly increased on introduction of amino groups in **6** and **9** and extension of conjugation in **8** and **9**, which led to the improved stability of the cation radicals formed by the removal of electron. The tetrasubstituted derivative **8** displayed an additional quasi-reversible oxidation process, which further supports the enhancement in oxidation propensity due to multiple substitutions on pyrene. The amine-substituted derivatives **6** and **9** exhibited a facile oxidation at the lower potentials attributed to the removal of electron from the amine unit. The oxidation due to the conjugation segment is cathodically shifted in **9** due to the presence of four amine units, which increases the electron density in the conjugation pathway.

dx.doi.org/10.1021/jo300285v | *J. Org. Chem.* 2012, 77, 3921–3932

Table 2. Absorption Data for Compounds 4−9 Recorded in Different Solvents

dye	λ_{max}, nm (ε_{max}, M^{-1} cm^{-1} × 10^3)							
	CH	TOL	$CHCl_3$	EA	THF	DCM	DMF	ACN
4	283 (26.0), 301 (21.5), 314 (27.4), 320 (21.9), 378 (42.9), 401 (46.1)	286 (34.7), 304 (28.2), 316 (35.3), 322 (33.1), 381 (52.3), 405 (53.9)	286 (35.9), 304 (30.7), 316 (37.6), 322 (35.4), 381 (59.6), 404 (64.9)	283 (31.2), 301 (26.9), 313 (32.7), 319 (26.9), 377 (51.8), 400 (57.4)	284 (31.7), 302 (26.8), 315 (33.4), 321 (29.0), 379 (53.2), 402 (58.8)	285 (33.2), 303 (29.1), 315 (35.4), 321 (32.5), 380 (57.0), 403 (63.6)	285 (34.6), 304 (31.3), 315 (38.3), 321 (35.9), 381 (61.5), 404 (71.7)	283 (36.9), 302 (34.2), 313 (41.1), 320 (34.2), 376 (67.7), 399 (77.8)
5	284, 330, 410, 418	286 (56.9), 332 (38.5), 414 (97.5), 424 (82.1)	286 (57.7), 332 (39.6), 414 (108.0), 421 (100.7)	283 (43.8), 329 (28.7), 409 (86.0), 419 (78.8)	285 (43.3), 330 (28.7), 411 (85.0), 421 (78.8)	285 (49.8), 331 (34.7), 412 (97.5), 424 (92.4)	286 (51.7), 331 (37.8), 413 (105.0), 427 (104.0)	283 (34.4), 329 (24.8), 408 (75.1), 420 (73.5)
6	285, 302, 392, 418	287 (33.5), 304 (34.4), 395 (54.2), 418 (46.8)	287 (35.4), 305 (37.3), 399 (59.7), 412 (57.6)	284 (31.3), 301 (32.0), 391 (54.0), 411 (50.3)	285 (31.7), 303 (32.8), 392 (53.6), 413 (50.4)	286 (29.8), 304 (32.3), 400 (50.8), 410 (50.4)	287 (36.5), 304 (38.9), 400 (61.2), 411 (61.4)	284 (30.3), 301 (31.9), 391 (51.9), 407 (51.3)
8	282 (66.9), 371 (116.5), 459 (62.0), 486 (68.5)	287(79.3), 374 (120.1), 464 (70.0), 488 (72.5)	285 (82.7), 375 (134.0), 465 (72.9), 491 (79.0)	283 (74.8), 372 (114.8), 461 (68.5), 488 (73.9)	285 (70.3), 375 (109.8), 464 (65.3), 492 (72.4)	285 (78.2), 374 (126.1), 465 (69.2), 492 (75.1)	288 (88.3), 377 (136.6), 468 (78.1), 496 (87.7)	na
9	308, 364, 410, 472, 500	310 (90.8), 364 (133.8), 413 (97.2), 476 (75.9), 503 (69.0)	314 (83.6), 370 (136.2), 411 (92.5), 476 (72.4), 503 (66.9)	306 (73.1), 364 (114.4), 408 (81.9), 473 (62.8), 502 (57.2)	306 (73.4), 364 (116.4), 412 (78.9), 477 (64.5), 506 (59.7)	310 (78.9), 368 (127.8), 410 (85.1), 476 (66.4), 504 (60.7)	306 (71.3), 368 (115.8), 411 (72.0), 479 (59.6), 506 (54.2)	na

The energies of frontier molecular orbitals (HOMO and LUMO) derived from the electrochemical and optical data are also listed in Table 4. Incorporation of triarylamine functionality raises the HOMO, while the tetrasubstitution is beneficial for stabilizing the LUMO. Combination of these two factors results in a relatively low band gap emitter **9**. The orbital energies observed for these materials, particularly the derivatives **6**, **8**, and **9** are more appropriate for facile charge injection at the electrode/molecular layer interfaces.

Theoretical Investigations. To gain further information about the electronic structure of the compounds, we have performed theoretical calculations using density functional theory[37] on approximated model compounds. To save the computational time the lengthy alkyl chains were removed in the model structures (**M4**−**M9**). It is opined that removal of alkyl groups from the molecules is not going to affect the parameters relevant for the discussion here. The isosurface plots of the frontier molecular orbitals of the selected model compounds of **6**, **8**, and **9** are shown in Figure 7, and the vertical transitions of all model compounds are listed in Table 5.

The LUMO of the compounds are invariably constituted by the pyrene unit in all of the compounds, while the HOMO is mainly on the pyrene unit and extended to the ethynylfluorene segment in the parent hydrocarbons **4**, **5**, and **8** or extended up to the amine nitrogen in compounds **6** and **9**. It is interesting note that the HOMO is spread over the diphenylamine fragment also in **6**, but the phenyl groups in the amine do not contribute for the construction of HOMO in **9**. The bathochromic shift in the absorption realized for the tetrasubstituted derivatives (**8** and **9**) on comparison to the monosubstituted derivatives (**4** and **6**) is easily understood on comparing the HOMO and LUMO of the respective molecules. The contribution of all four arms in the electronic delocalization strongly suggests that these molecules cannot be treated simply as cross-conjugated molecules and the π-acceptor ability of pyrene is enhanced on tetrasubstitution. The involvement of amine nitrogen in the HOMO for the compounds **6** and **9** further explains the slight red-shift observed for them on comparison to the parent hydrocarbons **4** and **8**. In general the HOMO to LUMO excitation in the compounds can be treated as a $\pi-\pi^*$ transition with the amine units in the compounds **6** and **9** rendering auxochromic effect. The trends observed in the peak positions and molar extinction coefficients of the compounds match well with the theoretical predictions (Tables 1 and 5). The absorption maxima observed for the compounds closely resemble to those computed using MPW1K model.[38] Thus, the computations based on this model can be utilized to predict functional properties of molecular materials at the design level and avoid the wastage of expensive chemicals on synthetic trials.

Thermal Properties. The thermal properties of compounds **4**−**9** were studied by thermogravimetric analysis (Table 4). All of the derivatives (**4**−**9**) exhibited excellent thermal stability, and the decomposition temperatures are in the range of 419−535 °C. The temperature corresponding to 5% weight loss for the dyes is in the range 394−467 °C. Among the dyes, **5** and **8** exhibited lower decomposition temperatures attributable to the fragile alkyl chains from in them. It is interesting to note that the dye **8** displayed improved thermal stability when compared to 1,3,6,8-tetrakis(9,9-dihexyl-9*H*-fluoren-2-yl)pyrene (377 °C).[29] It appears that the acetylene linkage present in **8** is acting as spacer and relieves the steric

dx.doi.org/10.1021/jo300285v | J. Org. Chem. 2012, 77, 3921−3932

Table 3. Emission Data for Compounds 4–9 Recorded in Different Solvents

	λ_{em}, nm					Stokes shift, cm^{-1}				
solvent	4	5	6	8	9	4	5	6	8	9
cyclohexane	407, 432	433, 457	436, 460	507, 542	524, 558	368	829	988	852	916
toluene	412, 436	438, 463	449	513, 549	535, 568	420	754	1652	999	1189
chloroform	413, 436	439, 464	486	514, 550	545	539	974	3696	911	1532
ethyl acetate	406, 431	433, 459	490	509, 545	545	369	772	3923	845	1572
THF	410, 434	437, 462	498	513, 549	552	485	978	4133	832	1647
dichloromethane	412, 435	439, 465	516	514, 551	567	542	806	5010	870	2205
DMF	412, 435	441, 465	565	518, 554	557	481	743	6632	856	1810
acetonitrile	408, 430	433, 457	557			553	715	6617		

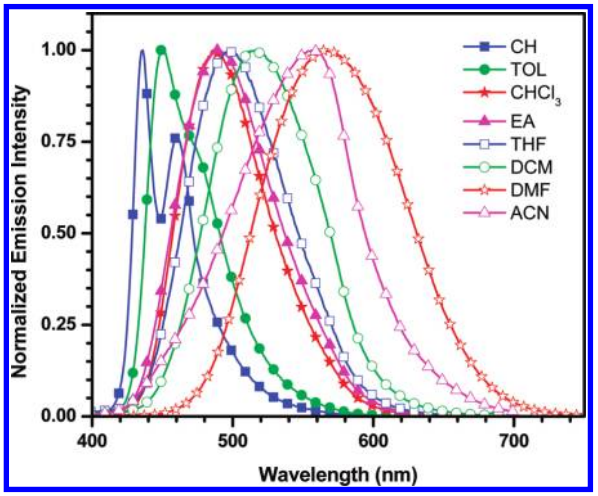

Figure 3. Emission spectra of **6** recorded in selected solvents of different polarity.

strain between the pyrene and fluorene units and contributes to the hike in stability. Highest thermal stability observed for the dyes **6** and **9** is attributed to the triarylamine chromophore in these molecules. Enhancement of thermal stability in molecular materials due to triarylamine chromophores has been well documented in the literature. Additionally, the role of fluorene unit in thermal stability is also evident on comparing **6** with the known derivative *N*,*N*-diphenyl-4-(pyren-1-yl)aniline (416 °C).[33]

Electroluminescent Properties. Two types of electroluminescent devices were fabricated using the newly developed materials [ITO/PEDOT:PSS/**4**, **5**, **6**, **8** or **9**/TPBi/LiF/Al (device I) and ITO/PEDOT:PSS/CBP:(**4**, **5**, **6**, **8** or **9**)/TPBi/LiF/Al (device II)], where ITO acts as anode, PEDOT:PSS as hole-injection layer, LiF as electron-injection layer, and Al as cathode. Compounds **4–9** were used as hole transporting and emitting material in device I, while host material 4,4′-bis(9*H*-carbazol-9-yl)biphenyl (**CBP**) doped with compounds **4–9** (10%) acts as ambipolar transporting and emitting layer in Device II. Figure 8 displays the I-V-L characteristics observed for devices I and II. The pertinent electroluminescent data for the dyes are listed in Table 6.

Devices II showed better performance statistics when compared to the corresponding devices I. From this it is clear that the materials are not effectively functioning as charge transporting emitting layer. The reason for the failure of devices I is mainly attributed to the lack of an amorphous state for the compounds, thus leading to poor quality films. The higher current density observed for devices I when compared to devices II also suggests that the charges are leaking at the

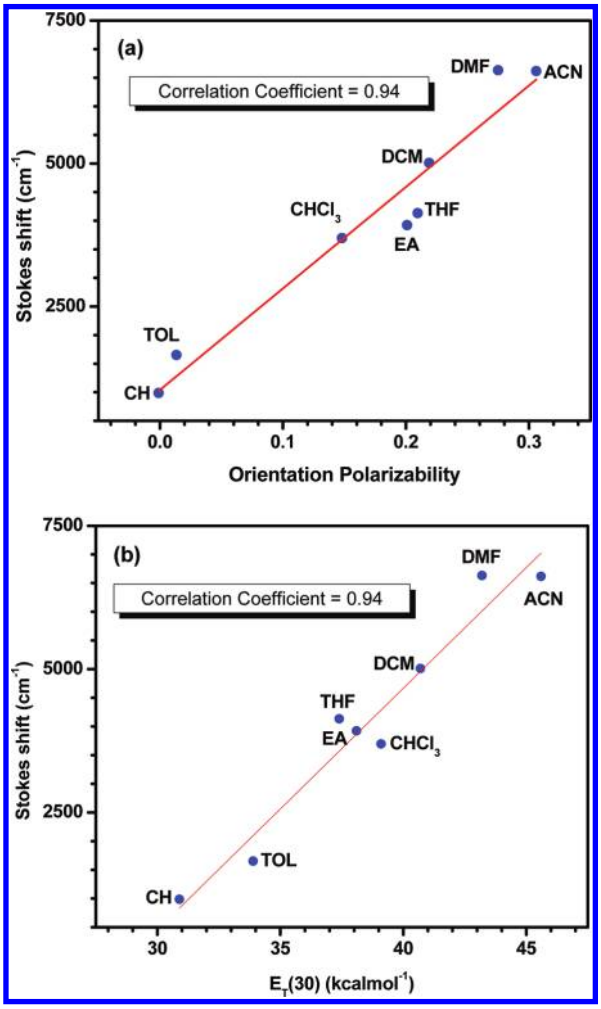

Figure 4. (a) Lippert–Mataga plot and (b) Stokes shift vs $E_T(30)$ plot for the dye **6**.

respective electrodes without recombining inside the molecular layer. The success of devices II is assigned to the favorable energy levels (Figure 9) of the compounds, which is suitable for the trapping of the excitons generated in the CBP layer. Among the dyes, the best performance was registered for **5** and **8** in terms brightness and efficiency for the device type II. These devices excel in performance compared to those reported based on 1,3,6,8-tetrakis(9,9-dihexyl-9*H*-fluoren-2-yl)pyrene.[29]

Figure 10 shows the EL spectra recorded for the devices II fabricated using dyes **4–9** at 100 cd/m^2 brightness. EL spectra of device II with compounds **4–9** were also recorded at the luminance of 1000 cd/m^2 and current density of 50 mA/m^2,

dx.doi.org/10.1021/jo300285v | J. Org. Chem. 2012, 77, 3921–3932

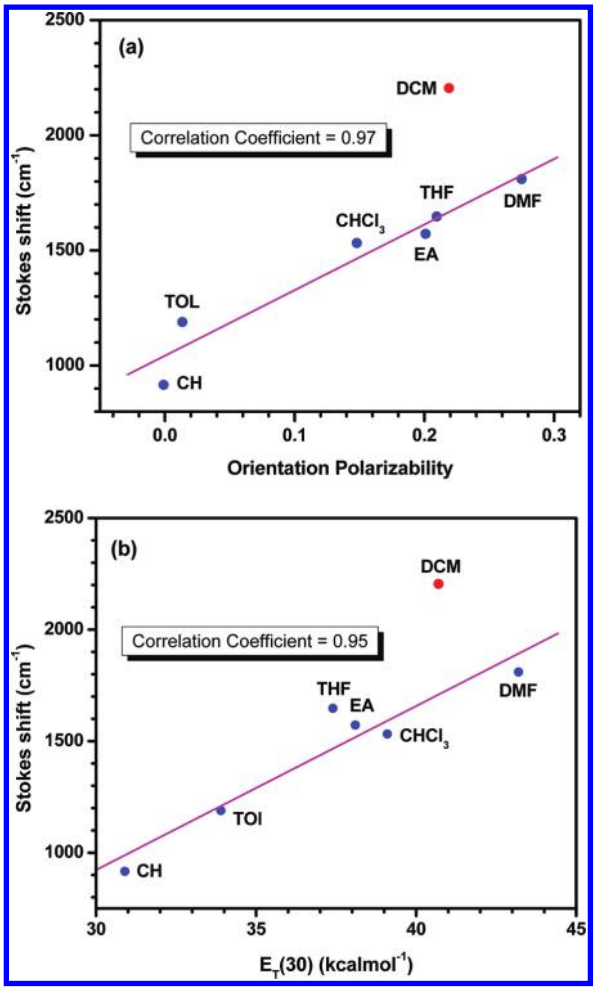

Figure 5. (a) Lippert–Mataga plot and (b) Stokes shift vs $E_T(30)$ plot for the dye **9**.

Table 4. Thermal and Electrochemical Data for Compounds 4–9

dye	T_{onset}, °C[a]	T_d, °C	T_m, °C	E_{ox} (ΔE_p), mV[b]	HOMO, eV[c]	LUMO, eV[d]	E_{0-0}, eV[e]
4	435	460	150	752	5.55	2.50	3.05
5	409	426	264	752	5.55	2.69	2.86
6	421	473	210	396 (65), 792 (66)	5.20	2.44	2.76
8	394	419	110	660 (56), 920 (66)	5.46	3.00	2.46
9	467	535	274	408 (71), 748 (61)	5.21	2.87	2.34

[a]Temperature corresponding to 5% weight loss. [b]Measured for 0.2 mM dichloromethane solutions and the potentials are quoted with reference to ferrocene internal standard. [c]HOMO = 4.8 + E_{ox}. [d]LUMO = HOMO − E_{0-0}. [e]Optical band gap obtained from the intersection of normalized absorption and emission spectra (optical edge).

and the details are provided in Table 6. The fwhm of the EL spectra remained unchanged over a wide luminance range and current density (see Table 6). It suggests that the hole and electron recombination is well confined within the CBP molecular layer that carries the emitter molecules. It is a common phenomenon that the EL spectrum of blue-emitting OLEDs shifts under different electric fields. This is mainly attributed to the difference in the charge carrier mobility in the employed organic layers, resulting in the shift of the emission

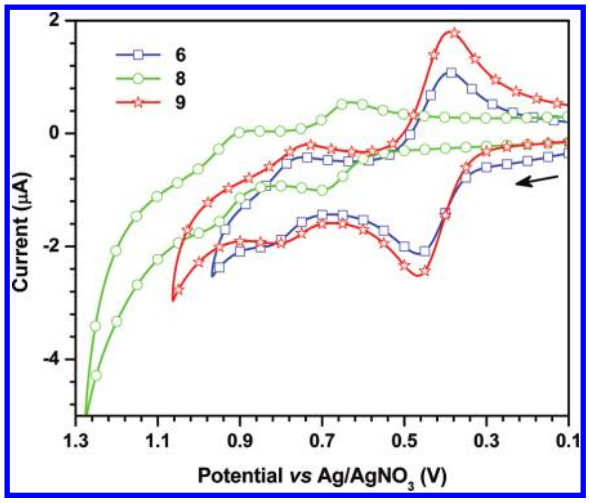

Figure 6. Cyclic voltammograms recorded for the dyes **6**, **8**, and **9**.

region. However, it is not the case for the present devices, i.e., the electroluminescence spectral peak remains constant over a wide luminance range (Table 7), which is of particular importance for the commercial full-color applications.

■ CONCLUSIONS

In summary we have developed pyrene-based molecular emitters featuring multiple fluorenylethnyl arms as potential candidates for organic light-emitting diodes. The compounds were synthesized by multifold palladium-catalyzed cross-coupling reactions and isolated in moderate to good yields. They were found to exhibit interesting photophysical properties that are highly dependent on the conjugation length and the nature of the terminal functional groups. Thus, the tetrasubstituted pyrene derivatives displayed red-shifted absorption and emission characteristics when compared to the monosubstituted pyrene derivatives due to the elongation of conjugation. The choice of acetylene linkage between the pyrene and fluorene chromophores has also been found to benefit the optical, electrochemical, and thermal properties of the compounds when compared to the derivatives in which fluorene and pyrene units are directly connected, which leads to sterically distorted and comparatively less conjugated molecules.[29] Incorporation of diphenylamine terminal groups red-shifts the absorption/emission profile and enhances the thermal stability. Compounds **4–9** were used as efficient dopant in multilayered organic light-emitting diodes with CBP as host. Device based on monosubstituted pyrene derivatives (**4–6**) showed bright blue emission, while the tetrasubstituted pyrene derivatives **8** and **9** exhibited yellow emission. The device based on dopant **8** displayed the highest maximum luminescence 4630 cd/m^2 with power efficiency 3.8 lm/W and current efficiency 7.1 cd/A at 100 cd/m^2, which is significantly better than the previously reported tetrasubstituted pyrene derivatives.[13a,29]

■ EXPERIMENTAL SECTION

General Methods. All commercial chemicals were used as received. Column chromatography was performed by using silica gel (100–200 mesh) as stationary phase. All solvents used in synthesis and spectroscopic measurements were distilled over appropriate drying and/or degassing reagents. ^{1}H and ^{13}C NMR spectra were recorded on a FT-NMR spectrometer operating at 500 and 125 MHz, respectively, in $CDCl_3$. Me_4Si (0.00 ppm) or residual signals for $CHCl_3$ (^{1}H NMR,

dx.doi.org/10.1021/jo300285v | J. Org. Chem. 2012, 77, 3921–3932

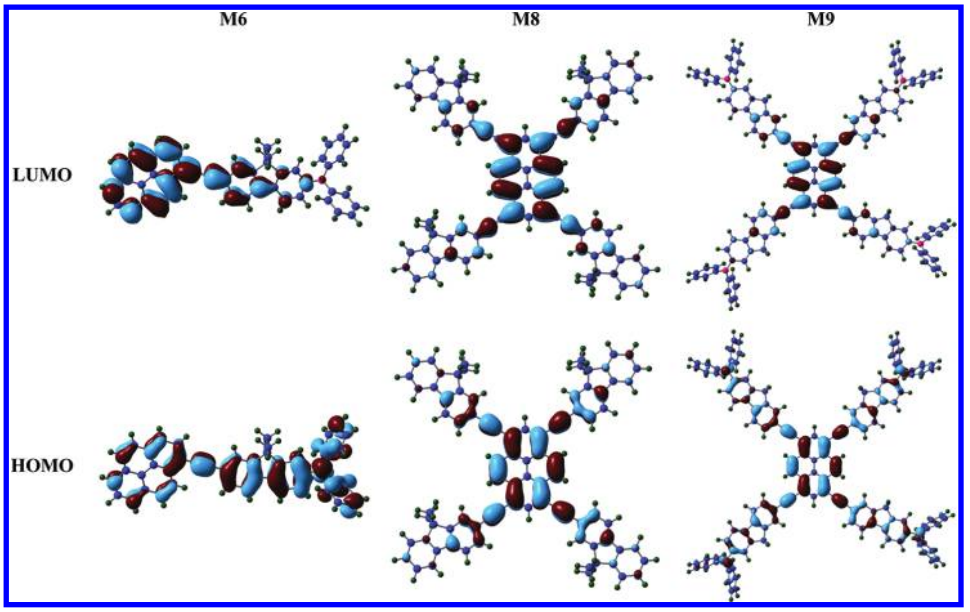

Figure 7. Computed isosurface plots of frontier molecular orbitals (HOMO and LUMO) for the model compounds of **6**, **8**, and **9**.

Table 5. Computed Vertical Transitions and Their Oscillator Strengths and Configurations[a]

	B3LYP			MPW1K		
compd	λ_{max}, nm	f	configuration	λ_{max}, nm	f	configuration
M4	420.2	1.3408	HOMO→LUMO (98%)	378.9	1.4747	HOMO→LUMO (95%)
	319.5	0.3473	HOMO→LUMO+1 (51%); HOMO-1→LUMO (37%)	294.2	0.4324	HOMO-1→LUMO (52%); HOMO→LUMO+1 (32%) HOMO→LUMO+2 (32%); HOMO→LUMO+4 (26%)
				256.6	0.1227	HOMO-2→LUMO (21%)
M5	477.0	2.4884	HOMO→LUMO (98%)	412.5	3.0971	HOMO→LUMO (82%); HOMO-1→LUMO+1(11%)
	376.8	0.4324	HOMO-1→LUMO+1 (89%)	362.8	0.1124	HOMO-1→LUMO (51%); HOMO→LUMO+1 (43%)
	333.0	0.1610	HOMO→LUMO+2 (44%); HOMO-2→LUMO (42%)	287.7	0.1146	HOMO-2→LUMO (52%); HOMO −1→LUMO+1 (15%)
				285.4	0.1227	HOMO→LUMO+2 (56%); HOMO-1→LUMO+1 (15%)
				275.2	0.2748	HOMO-2→LUMO+1 (33%); HOMO-1→LUMO+2 (25%) HOMO-5→LUMO (10%)
M6	465.4	1.2439	HOMO→LUMO (98%)	393.8	1.9664	HOMO→LUMO (82%)
	395.6	0.5507	HOMO-1→LUMO (89%)	299.1	0.2226	HOMO→LUMO+1 (52%); HOMO→LUMO+2 (11%)
	348.8	0.1371	HOMO→LUMO+2 (26%); HOMO-2→LUMO (18%); HOMO-3→LUMO (15%); HOMO→LUMO+1 (15%); HOMO-1→LUMO+1(13%)	277.9	0.1961	HOMO-1→LUMO (11%) HOMO-2→LUMO (45%); HOMO-1→LUMO+1 (28%)
				274.2	0.2332	HOMO→LUMO+4 (64%); HOMO-1→LUMO+4 (29%)
	313.0	0.1263	HOMO-1→LUMO+1 (35%); HOMO-2→LUMO (32%); HOMO-3→LUMO (14%)			
	312.1	0.2024	HOMO→LUMO+4 (88%)			
M8	567.7	1.6860	HOMO →LUMO (99%)	495.3	1.9341	HOMO→LUMO (95%)
	452.7	0.3131	HOMO-1→LUMO (80%); HOMO→LUMO+1 (16%)	377.4	0.5914	HOMO-1→LUMO (68%); HOMO-5→LUMO (10%)
				357.2	2.9266	HOMO→LUMO+1 (67%); HOMO-1→LUMO (15%)
	415.1	2.2161	HOMO→LUMO+1 (78%); HOMO-1→LUMO (18%)			
M9	604.9	1.9035	HOMO→LUMO (98%)	508.6	2.3823	HOMO→LUMO (91%)
	534.2	0.4966	HOMO-1→LUMO (97%)	404.1	2.3112	HOMO-1→LUMO (64%); HOMO-5→LUMO (13%)
	532.7	0.3402	HOMO-2→LUMO (97%)			HOMO-2→LUMO (10%)

[a]Orbital contributions below 10% are omitted.

δ = 7.26; ^{13}C NMR, δ = 77.36 ppm) or DMSO (^{1}H NMR, δ = 2.5 ppm; ^{13}C NMR δ = 40.45 ppm) served as internal standard. IR spectra were measured on a FT-IR spectrometer. The electronic absorption spectra were obtained with a UV−vis spectrophotometer. High resolution mass spectra were measured in an electron spray ionization (ESI) mass spectrometer operating in positive ion mode. Emission spectra were recorded spectrofluorimeter by using freshly prepared dilute solutions. The fluorescence quantum yields (Φ_F) were determined using the formula $\Phi_s = (\Phi_r \times A_r \times I_s \times \eta_s^2)/(A_s \times I_r \times \eta_r^2)$ where A is the absorbance at the excitation wavelength, I is the

dx.doi.org/10.1021/jo300285v | J. Org. Chem. 2012, 77, 3921−3932

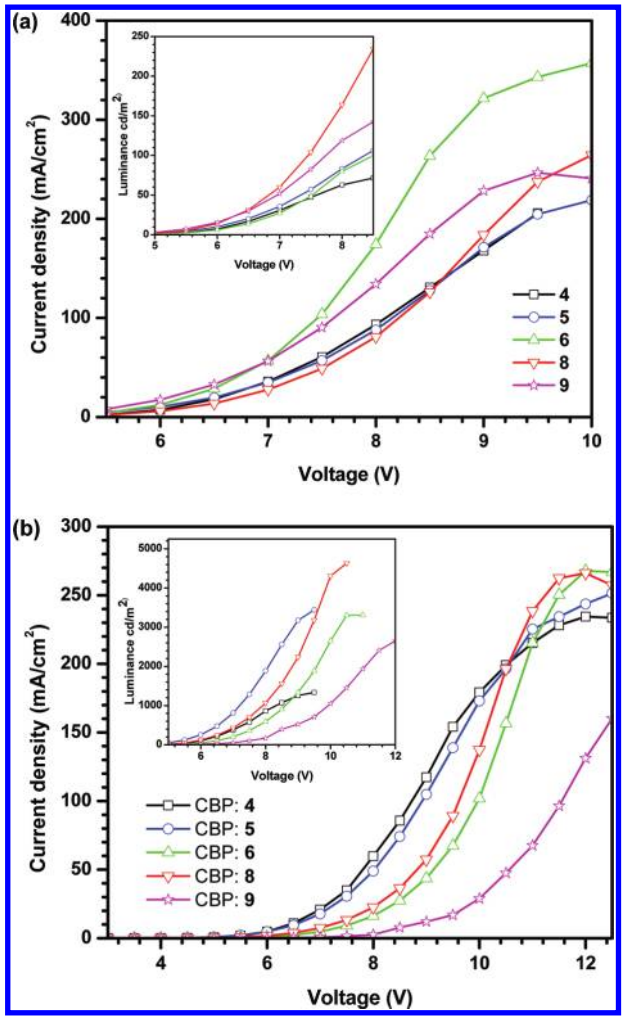

Figure 8. I-V-L characteristics observed for the devices (a) I and (b) II.

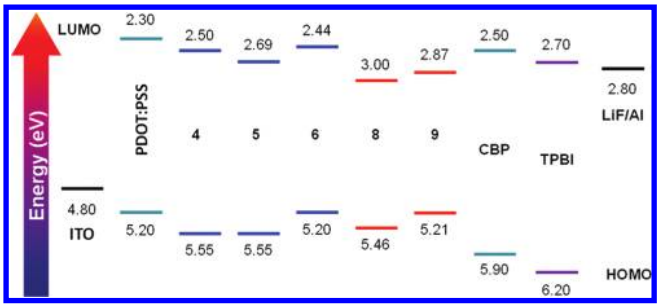

Figure 9. Energy level alignment in the materials used for the fabrication of devices.

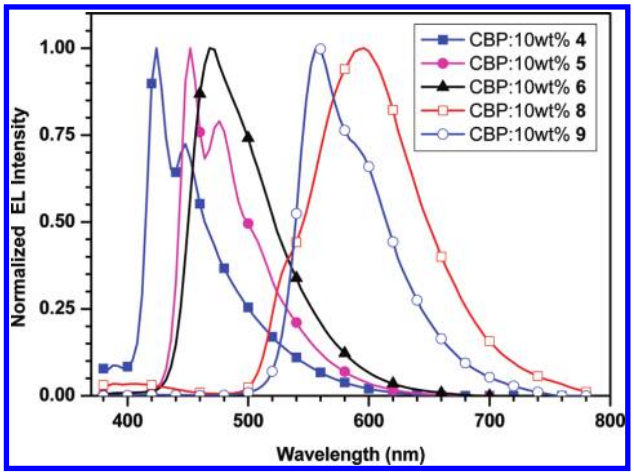

Figure 10. EL spectra measured at100 cd/m^2 for the devices II using 10% dyes **4**–**9** with CBP host.

integrated area under the fluorescence curve, and η is the refraction index. Subscripts r and s refer to the reference and to the sample of unknown quantum yield, respectively. Coumarin-6 in ethanol (Φ_F = 0.78) and coumarin-1 in ethyl acetate (Φ_F = 0.99) were taken as the reference.[24] Cyclic voltammetry experiments were performed with a electrochemical analyzer. All measurements were carried out at room temperature with a conventional three-electrode configuration consisting of a glassy carbon working electrode, a platinum wire auxiliary, and a nonaqueous acetonitrile Ag/$AgNO_3$ reference electrode. The $E_{1/2}$ values were determined as $(E_p^a + E_p^c)/2$, where E_p^a and E_p^c are the anodic and cathodic peak potentials, respectively. The potential are quoted against ferrocene internal standard. The solvent in all experiments was dichloromethane and the supporting electrolyte was 0.1 M tetrabutylammonium hexafluorophosphate. Thermogravimetric analyses (TGA) were performed under nitrogen atmosphere at heating rate of 10 °C/min.

1-Bromopyrene (**1**) and 1,3,6,8-tetrabromopyrene (**2**) were made by reported procedure.[39] Precursor acetylenes **3a**, **3b**, and **3d** were synthesized by known literature procedure.[40]

Synthesis of 9,9-Diethyl-7-ethynyl-*N*,*N*-diphenyl-9*H*-fluoren-2-amine (3c). A mixture of 7-bromo-9,9-diethyl-*N*,*N*-diphenyl-9*H*-fluoren-2-amine (5.0 g, 10.68 mmol), 2-methylbut-3-yn-2-ol (1.07 g, 12.8 mmol), $Pd(PPh_3)_2Cl_2$ (75 mg, 0.11 mmol), PPh_3 (56 mg, 0.21 mmol), and CuI (21 mg, 0.11 mmol) were mixed in triethylamine (100 mL) under nitrogen atmosphere. The resulting mixture was stirred and heated at 100 °C for 24 h. After completion of the reaction,

Table 6. Electroluminescence Characteristics of Devices I and II Based on Compounds 4–9

		at 100/1000 cd/m^2				
material	driving voltage (V) at 10 cd/m^2	power efficiency (lm/W)	current efficiency (cd/A)	EQE (%)	max luminance (cd/m^2)	CIE
4	6.1				65	(0.19, 0.23)
5	6.0	0.03/0.09			111	(0.20, 0.34)
6	6.3				99	(0.20, 0.34)
8	6.1	0.09/0.21			282	(0.48, 0.43)
9	5.9	0.09/0.04			143	(0.50, 0.46)
4 + CBP	5.0	1.1/0.5	2.2/1.3	2.6/1.2	1340	(0.16, 0.12)
5 + CBP	4.3	3.6/1.9	6.0/4.4	4.5/3.3	3440	(0.16, 0.21)
6 + CBP	5.2	2.3/1.2	4.7/3.3	2.6/1.9	3310	(0.17, 0.29)
8 + CBP	4.8	3.8/1.9	7.1/4.8	3.2/2.1	4630	(0.52, 0.47)
9 + CBP	5.7	3.1/1.2	7.3/3.7	2.3/11	2650	(0.48, 0.51)

dx.doi.org/10.1021/jo300285v | J. Org. Chem. 2012, 77, 3921–3932

Table 7. Emission and Electroluminescence Spectral Data of Compounds 4−9

	λ_{em} (nm)[a]		λ_{EL} (nm)[b]			
compound	dcm	thin film	at max luminance[c]	at 100 cd/m^{2d}	at 1000 cd/m^{2d}	at 50 mA/m^{2d}
4	412, 435	496	480	424, 448	424, 448	424, 448
5	439, 465	486, 505	480	452, 476	452, 476	452, 476
6	516	495	484	468	468	468
8	514, 551	587	588	596, 528 (sh)	588, 528 (sh)	588, 528 (sh)
9	567	581	576	556, 592 (sh)	556, 592 (sh)	556, 592 (sh)

[a]Emission wavelength. [b]Electroluminescence wavelength for OLED device. [c]Wavelength for device I (without CBP). [d]Wavelength for device II (doping with CBP).

the mixture was poured into water and extracted with ethyl acetate. The organic extract was washed with brine solution and dried over Na_2SO_4. Finally, the solvent was removed under vacuum to yield a yellow residue, which was purified by column chromatography as a yellow liquid (5.2 g, 55%) that further undergo cleavage reaction with KOH and toluene to produce the acetylene **3c**. Yellow solid. Yield 3.58 (71%); ^{1}H NMR ($CDCl_3$, 500 MHz) δ 7.57−7.55 (m, 2 H), 7.46 (dd, J = 6.5, 1.5 Hz, 1 H), 7.42 (d, J = 1.0 Hz, 1 H), 7.28−7.25 (m, 4 H), 7.13−7.11 (m, 4 H), 7.09 (d, J = 2.0 Hz, 1 H), 7.05−7.01 (m, 3 H), 3.12 (s, 1 H), 1.95−1.87 (m, 4 H), 0.35 (t, J = 7.5 Hz, 6 H); ^{13}C NMR ($CDCl_3$, 125 MHz) δ 151.7, 149.9, 147.9, 147.8, 142.2, 135.7, 131.3, 126.5, 123.5, 122.7, 120.8, 119.3, 119.0, 118.9, 84.8, 56.1, 32.6, 8.5.

Synthesis of 1-((9,9-Diethyl-9*H*-fluoren-2-yl)ethynyl)pyrene (4). A mixture of 1-bromopyrene (2.82 g, 10 mmol), 9,9-diethyl-2-ethynyl-9*H*-fluorene (**3a**) (2.95 g, 12 mmol), $Pd(PPh_3)_2Cl_2$ (70 mg, 0.1 mmol), PPh_3 (52 mg, 0.2 mmol), and CuI (20 mg, 0.1 mmol) were mixed in triethylamine (100 mL) under nitrogen atmosphere. The resulting mixture was stirred and heated at 100 °C for 24 h. After completion of the reaction, the mixture was poured into water and extracted with ethyl acetate. The organic extract was washed with brine solution and dried over Na_2SO_4. Finally, the solvent was removed under vacuum to yield a yellow residue, which was purified by column chromatography. Yellow solid. Yield 2.2 g (48%); mp 150−152 °C; IR (KBr, cm^{-1}) 2191 ($\nu_{C\equiv C}$); ^{1}H NMR ($CDCl_3$, 500 MHz) δ 8.75 (d, J = 9.0 Hz, 1 H), 8.26−8.21 (m, 4 H), 8.17−8.03 (m, 4 H), 7.79−7.70 (m, 4 H), 7.39−7.36 (m, 3 H), 2.12 (q, J = 7.5 Hz, 4 H), 0.39 (t, J = 7.5 Hz, 6 H); ^{13}C NMR ($CDCl_3$, 125 MHz) δ 150.3, 150.2, 142.1, 140.9, 131.9, 131.3, 131.21, 131.17, 130.9, 129.7, 128.3, 128.1, 127.6, 127.3, 127.0, 126.3, 126.1, 125.7, 125.63, 125.57, 124.62, 124.59, 124.4, 123.0, 121.8, 120.1, 119.8, 118.1, 96.3, 88.7, 32.8, 8.6; HRMS calcd for $C_{35}H_{26}$ m/z 446.2035, found 446.2034. Anal. Calcd for $C_{35}H_{26}$: C, 94.13; H, 5.87. Found: C, 93.95; H, 5.69.

Synthesis of 1,1′-((9,9-Dibutyl-9*H*-fluorene-2,7-diyl)bis-(ethyne-2,1-diyl))dipyrene (5). Compound **5** was prepared from **1** and **3b** by following a procedure similar to that described above for **4**. Yellow solid. Yield 2.6 g (35%); mp 264−266 °C; IR (KBr, cm^{-1}) 2187 ($\nu_{C\equiv C}$); ^{1}H NMR ($CDCl_3$, 500 MHz) δ 8.76 (d, J = 9.0 Hz, 2 H), 8.29−8.22 (m, 8 H), 8.18 (d, J = 8.0 Hz, 2 H), 8.13−8.04 (m, 6 H), 7.81 (d, J = 8.0 Hz, 2 H), 7.77 (dd, J = 1.5, 6.5 Hz, 2 H), 7.73 (s, 2 H), 2.15−2.12 (m, 4 H), 1.21−1.17 (m, 4 H), 0.89−0.69 (m, 10 H); ^{13}C NMR ($CDCl_3$, 125 MHz) δ 151.4, 140.9, 131.9, 131.33, 131.29, 131.2, 131.0, 129.7, 128.4, 128.2, 127.3, 126.3, 126.0, 125.7, 125.6, 124.64, 124.60, 124.4, 122.3, 120.2, 118.0, 96.3, 89.2, 55.4, 40.4, 29.7, 26.0, 23.2, 14.0; HRMS calcd for $C_{57}H_{42}$ m/z 726.3287, found 726.3283. Anal. Calcd for $C_{57}H_{42}$: C, 94.18; H, 5.82. Found: C, 94.01; H, 5.70.

Synthesis of 9,9-Diethyl-*N*,*N*-diphenyl-7-(pyren-1-ylethynyl)-9*H*-fluoren-2-amine (6). Compound **6** was prepared from **1** and **3c** by following a procedure similar to that described above for **4**. Yellow solid. Yield 3.5 g (57%); mp 210−212 °C; IR (KBr, cm^{-1}) 2195 ($\nu_{C\equiv C}$); ^{1}H NMR ($CDCl_3$, 500 MHz) δ 8.74 (d, J = 9.0 Hz, 1 H), 8.25−8.20 (m, 4 H), 8.15 (d, J = 8.0 Hz, 1 H), 8.11−8.03 (m, 3 H), 7.71−7.65 (m, 3 H), 7.61 (d, J = 8.5 Hz, 1 H), 7.30−7.27 (m, 4 H), 7.17−7.14 (m, 5 H), 7.09−7.03 (m, 3 H), 2.05 (m, 2 H), 1.96 (m, 2 H), 0.44 (t, J = 7.5 Hz, 6 H); ^{13}C NMR ($CDCl_3$, 125 MHz) δ 151.8, 150.1, 148.0, 147.8, 141.9, 135.9, 131.9, 131.3, 131.18, 131.16, 131.0, 129.6, 129.3, 128.3, 128.1, 127.3, 126.3, 126.0, 125.7, 125.63, 125.57, 124.64, 124.60, 124.4, 124.2, 124.1, 123.6, 122.9, 122.8, 120.9, 120.8, 119.2, 119.1, 118.2, 96.5, 88.7, 56.3, 32.8, 8.7, 8.6; HRMS calcd for $C_{47}H_{35}N$ m/z 613.2770, found 613.2769. Anal. Calcd for $C_{47}H_{35}N$: C, 91.97; H, 5.75; N, 2.28. Found: C, 91.68; H, 5.62; N, 2.14.

Synthesis of 1,3,6,8-Tetrakis((9,9-diethyl-9*H*-fluoren-2-yl)-ethynyl)pyrene (7). Compound **7** was prepared from **2** and **3a** by following a procedure similar to that described above for **4**. Orange solid. Yield 10.3 g (87%); mp >360 °C; IR (KBr, cm^{-1}) 2195 ($\nu_{C\equiv C}$); ^{1}H NMR ($CDCl_3$, 500 MHz) δ 8.88 (s, 4 H), 8.55 (s, 2 H), 7.81−7.71 (m, 16 H), 7.39−7.38 (m, 12 H), 2.18−2.08 (m, 16 H), 0.40 (t, J = 7.0 Hz, 24 H); ^{13}C NMR ($CDCl_3$, 125 MHz) δ 149.3, 149.2, 141.3, 139.8, 130.7, 129.9, 126.7, 126.03, 125.96, 125.2, 122.0, 120.4, 119.1, 118.8, 118.2, 99.0, 96.3, 86.9, 55.3, 45.2, 31.8, 7.5; HRMS calcd for $C_{92}H_{74}$ m/z 1178.5791, found 1178.5786. Anal. Calcd for $C_{92}H_{74}$: C, 93.68; H, 6.32. Found: C, 93.34; H, 6.08.

Synthesis of 1,3,6,8-Tetrakis((9,9-di(octan-3-yl)-9*H*-fluoren-2-yl)ethynyl)pyrene (8). Compound **8** was prepared from **2** and **3d** by following a procedure similar to that described above for **4**. Red solid. Yield: 10.3 g (80%); mp: 110−112 °C; IR (KBr, cm^{-1}) 2195 ($\nu_{C\equiv C}$); ^{1}H NMR ($CDCl_3$, 500 MHz): δ = 8.87 (s, 4 H), 8.55−8.57 (m, 2 H), 7.70−7.80 (m, 16 H), 7.43−7.47 (m, 4 H), 7.31−7.39 (m, 8 H), 2.09−2.10 (m, 16 H), 1.02−0.82 (m, 78 H), 0.80−0.72 (m, 10 H), 0.56−0.65 (m, 32 H); ^{13}C NMR ($CDCl_3$, 125 MHz): δ = 150.89, 150.85, 150.8, 142.1, 140.61, 140.59, 133.8, 131.8, 130.9, 130.80, 130.75, 129.1, 128.3, 127.4, 127.3, 127.2, 127.1, 127.0, 126.9, 124.4, 124.20, 124.17, 121.0, 120.93, 120.88, 120.1, 119.8, 119.3, 97.4, 87.7, 55.0, 44.8, 44.5, 44.5, 34.7, 33.8, 33.73, 33.66, 33.6, 32.0, 29.73, 29.70, 29.4, 28.2, 27.08, 27.06, 22.8, 22.7, 14.21, 14.15, 14.0, 10.43, 10.41, 10.4. HRMS calcd for $C_{140}H_{170}$ m/z 1851.3303, found 1851.3294. Anal. Calcd for $C_{140}H_{170}$: C, 90.75; H, 9.25. Found: C, 90.59; H, 9.12.

Synthesis of 7,7′,7″,7‴-(Pyrene-1,3,6,8-tetrayltetrakis-(ethyne-2,1-diyl))tetrakis(9,9-diethyl-*N*,*N*-diphenyl-9*H*-fluoren-2-amine) (9). Compound **9** was prepared from **2** and **3c** by following a procedure similar to that described above for **4**. Orange solid. Yield 14.4 g (78%); mp 274−276 °C; IR (KBr, cm^{-1}) 2192 ($\nu_{C\equiv C}$); ^{1}H NMR ($CDCl_3$, 500 MHz) δ 8.85 (s, 4 H), 8.51 (s, 2 H), 7.73−7.65 (m, 11 H), 7.61 (d, J = 8.5 Hz, 4 H), 7.28−7.29 (m, 12 H), 7.13−7.16 (m, 22 H), 7.00−7.09 (m, 15 H), 2.09−2.05 (m, 8 H), 1.94−1.98 (m, 8 H), 0.42−0.45 (m, 24 H); ^{13}C NMR ($CDCl_3$, 125 MHz) δ 151.8, 150.1, 147.9, 147.8, 142.2, 135.8, 133.7, 131.7, 131.1, 129.2, 126.9, 126.0, 124.3, 123.9, 123.5, 122.7, 120.8, 120.5, 119.22, 119.17, 119.0, 97.5, 87.9, 56.3, 32.7, 29.7, 8.6. HRMS calcd for $C_{140}H_{112}N_4$ [M + 2H] 1848.8887, found 1848.8871. Anal. Calcd for $C_{140}H_{110}N_4$: C, 90.97; H, 6.00; N, 3.03. Found: C, 90.78; H, 5.77; N, 2.86.

OLED Fabrication and Performance Evaluation. The OLED devices for the dyes **4**−**9** were fabricated on a precleaned glass substrate containing a 125 nm layer indium tin oxide as anode, 35 nm poly(3,4-ethylene-dioxythiophene)-poly(styrenesulfonate) (PEDOT:PSS) as hole-injection layer (HIL), emissive layer (EML), 32 nm 1,3,5-tris(*N*-phenylbenzimidazol-2-yl)benzene (TPBi) as electron transporting layer (ETL), a 0.7 nm LiF electron injection layer (EIL), and a 150 nm Al layer as cathode. The aqueous solution of PEDOT:PSS was spin coated at 4000 rpm for 20 s to form a 40 nm HIL layer. The dyes **4**−**9** doped in 4,4′-bis(9*H*-carbazol-9-yl)biphenyl (CBP) were deposited by spin-coating at 2500 rpm for 20 s and served as emissive layer. Subsequently, lithium fluoride and aluminum cathode were thermally evaporated at 1.0 × 10^{-5} Torr.

Computational Methods. All computations were performed with the Gaussian 09 program package.[41] The ground-state geometries were fully optimized without any symmetry constrains at the DFT level with Becke's three parameters hybrid functional and Lee, Yang and Parr's correlational functional B3LYP[42] and MPW1K[38] using the 6-31G* basis set on all atoms. Vibrational analyses on the optimized structures

dx.doi.org/10.1021/jo300285v | J. Org. Chem. 2012, 77, 3921−3932

were performed to confirm the structure. The excitation energies and oscillator strengths for the lowest 10 singlet−singlet transitions at the optimized geometry in the ground state were obtained by TD-DFT calculations using the same basis set as for the ground state using the same theory level.

■ ASSOCIATED CONTENT

Supporting Information

^{1}H and ^{13}C NMR spectra of the newly synthesized compounds, optical spectra of the compounds recorded in different solvents, and Cartesian coordinates of the theoretically modeled structures. This material is available free of charge via the Internet at http://pubs.acs.org.

■ AUTHOR INFORMATION

Corresponding Author

*Fax: +91-1332-286202. Tel: +91-1332-285376. E-mail:krjt8fcy@iitr.ernet.in.

Notes

The authors declare no competing financial interest.

■ ACKNOWLEDGMENTS

K.R.J.T. is thankful to Council of Scientific and Industrial Research, New Delhi for financial support (01(1799)/11/EMR-II). The Advanced Instrumentation Research Facility at Jawaharlal Nehru University at New Delhi is acknowledged for providing access to ESI mass spectrometer.

■ REFERENCES

(1) (a) Tang, C. W.; VanSlyke, S. A. *Appl. Phys. Lett.* **1987**, *51*, 913−915. (b) Sun, Y.; Giebink, N. C.; Kanno, H.; Ma, B.; Thompson, M. E.; Forrest, S. R. *Nature* **2006**, *440*, 908−912. (c) Hancock, J. M.; Gifford, A. P.; Zhu, Y.; Lou, Y.; Jenekhe, S. A. *Chem. Mater.* **2006**, *18*, 4924−4932. (d) Burn, P. L.; Lo, S. C.; Samuel, D. W. *Adv. Mater.* **2007**, *19*, 1675−1688. (e) Lyu, Y. Y.; Kwak, J.; Kwon, O.; Lee, S. H.; Kim, D.; Lee, C.; Char, K. *Adv. Mater.* **2008**, *20*, 2720−2729. (f) Tonzola, C. J.; Kulkarni, A. P.; Gifford, A. P.; Kaminsky, W.; Jenekhe, S. A. *Adv. Funct. Mater.* **2007**, *17*, 863−874. (g) Tao, S.; Zhou, Y.; Lee, C. S.; Zhang, X.; Lee, S. T. *Chem. Mater.* **2010**, *22*, 2138−2141. (h) Duan, L.; Hou, L.; Lee, T. W.; Qiao, J.; Zhang, D.; Dong, G.; Wang, L.; Qiu, Y. J. *J. Mater. Chem.* **2010**, *20*, 6392−6407.

(2) (a) Zhan, X.; Tan, Z. A.; Domercq, B.; An, Z.; Zhang, X.; Barlow, S.; Li, Y.; Zhu, D.; Kippelen, B.; Marder, S. R. *J. Am. Chem. Soc.* **2007**, *129*, 7246−7247. (b) Martinson, A. B. F.; Hamann, T. W.; Pellin, M. J.; Hupp, J. T. *Chem.—Eur. J.* **2008**, *14*, 4458−4467. (c) Velusamy, M.; Huang, J.-H.; Hsu, Y.-C.; Chou, H.-H.; Ho, K.-C.; Wu, P.-L.; Chang, W.-H.; Lin, J. T.; Chu, C.-W. *Org. Lett.* **2009**, *11*, 4898−4901. (d) Ning, Z.; Tian, H. *Chem. Commun.* **2009**, 5483−5495. (e) Hagfeldt, A.; Boschloo, G.; Sun, L.; Kloo, L.; Pettersson, H. *Chem. Rev.* **2010**, *110*, 6595−6663. (f) Clifford, J. N.; Martínez-Ferrero, E.; Viterisi, A.; Palomares, E. *Chem. Soc. Rev.* **2011**, *40*, 1635−1646. (g) Zhan, X. W.; Facchetti, A.; Barlow, S.; Marks, T. J.; Ratner, M. A.; Wasielewski, M. R.; Marder, S. R. *Adv. Mater.* **2011**, *23*, 268−284.

(3) (a) Sundar, V. C.; Zaumseil, J.; Podzorov, V.; Menard, E.; Willett, R. L.; Someya, T.; Gershenson, M. E.; Rogers, J. A. *Science* **2004**, *303*, 1644−1647. (b) Sun, Y. M.; Liu, Y. Q.; Zhu, D. B. *J. Mater. Chem.* **2005**, *15*, 53−65. (c) Mas-Torrent, M.; Rovira, C. *J. Mater. Chem.* **2006**, *16*, 433−436. (d) Jung, B. J.; Tremblay, N. J.; Yeh, M.-L.; Katz, H. E. *Chem. Mater.* **2011**, *23*, 568−582. (e) Niimi, K.; Shinamura, S.; Osaka, I.; Miyazaki, E.; Takimiya, K. *J. Am. Chem. Soc.* **2011**, *133*, 8732−8739.

(4) (a) Lee, S. K.; Yang, W. J.; Choi, J. J.; Kim, C. H.; Jeon, S.-J.; Cho, B. R. *Org. Lett.* **2005**, *7*, 323−326. (b) Mongin, O.; Porrès, L.; Charlot, M.; Katan, C.; Blanchard-Desce, M. *Chem.—Eur. J.* **2007**, *13*, 1481−1498. (c) Sumalekshmy, S.; Henary, M. M.; Siegel, N.; Lawson, P. V.; Wu, Y. G.; Schmidt, K.; Bredas, J.-L.; Perry, J. W.; Fahrni, C. J. *J. Am. Chem. Soc.* **2007**, *129*, 11888−11889. (d) He, G. S.; Tan, L.-S.; Zheng, Q.; Prasad, P. N. *Chem. Rev.* **2008**, *108*, 1245−1330.

(5) (a) Terenziani, F.; Painelli, A.; Katan, C.; Charlot, M.; Blanchard-Desce, M. *J. Am. Chem. Soc.* **2006**, *128*, 15742−15755. (b) Terenziani, F.; D'Avino, G.; Painelli, A. *ChemPhysChem* **2007**, *8*, 2433−2444. (c) Rizzo, F.; Cavazzini, M.; Righetto, S.; De Angelis, F.; Fantacci, S.; Quici, S. *Eur. J. Org. Chem.* **2010**, 4004−4016. (d) Nakano, M.; Kishi, R.; Yoneda, K.; Inoue, Y.; Inui, T.; Shigeta, Y.; Kubo, T.; Champagne, B. *J. Phys. Chem. A* **2011**, *115*, 8767−8777.

(6) (a) Tao, S.; Peng, Z.; Zhang, X.; Wang, P.; Lee, C.-S.; Lee, S.-T. *Adv. Funct. Mater.* **2005**, *15*, 1716−1721. (b) Promarak, V.; Punkvuang, A.; Sudyoadsuk, T.; Jungsuttiwong, S.; Saengsuwan, S.; Keawin, T.; Sirithip, K. *Tetrahedron* **2007**, *63*, 8881−8890. (c) Grisorio, R.; Melcarne, G.; Suranna, G. P.; Mastrorilli, P.; Nobile, C. F.; Cosma, P.; Fini, P.; Colella, S.; Fabiano, E.; Piacenza, M.; Della Sala, F.; Ciccarella, G.; Mazzeo, M.; Gigli, G. *J. Mater. Chem.* **2010**, *20*, 1012−1018. (d) Zhang, T.; Liu, D.; Wang, Q.; Wang, R. J.; Ren, H. C.; Li, J. Y. *J. Mater. Chem.* **2011**, *21*, 12969−12976. (e) Zhu, M. R.; Ye, T. L.; Li, C. G.; Cao, X. S.; Zhong, C.; Ma, D. G.; Qin, J. G.; Yang, C. L. *J. Phys. Chem. C* **2011**, *115*, 17965−17972.

(7) (a) Wang, J.; Wan, W.; Jiang, H.; Gao, Y.; Jiang, X.; Lin, H.; Zhao, W.; Hao, J. *Org. Lett.* **2010**, *12*, 3874−3877. (b) Wee, K. R.; Han, W. S.; Kim, J. E.; Kim, A. L.; Kwon, S.; Kang, S. O. *J. Mater. Chem.* **2011**, *21*, 1115−1123. (c) Zhu, M. R.; Wang, Q. A.; Gu, Y.; Cao, X. S.; Zhong, C.; Ma, D. G.; Qin, J. G.; Yang, C. L. *J. Mater. Chem.* **2011**, *21*, 6409−6415. (d) Huang, J. H.; Su, J. H.; Li, X.; Lam, M. K.; Fung, K. M.; Fan, H. H.; Cheah, K. W.; Chen, C. H.; Tian, H. *J. Mater. Chem.* **2011**, *21*, 2957−2964. (e) Cho, I.; Kim, S. H.; Kim, J. H.; Park, S.; Park, S. Y. *J. Mater. Chem.* **2012**, *22*, 123−129.

(8) (a) Wurthner, F.; Stolte, M. *Chem. Commun.* **2011**, *47*, 5109−5115. (b) Battagliarin, G.; Zhao, Y.; Li, C.; Müllen, K. *Org. Lett.* **2011**, *13*, 3399−3401.

(9) (a) Maeda, H.; Maeda, T.; Mizuno, K.; Fujimoto, K.; Shimizu, H.; Inouye, M. *Chem.—Eur. J.* **2006**, *12*, 824−831. (b) Shimizu, H.; Fujimoto, K.; Furusyo, M.; Maeda, H.; Nanai, Y.; Mizuno, K.; Inouye, M. *J. Org. Chem.* **2007**, *72*, 1530−1533. (c) Xia, R. D.; Lai, W. Y.; Levermore, P. A.; Huang, W.; Bradley, D. D. C. *Adv. Funct. Mater.* **2009**, *19*, 2844−2850. (d) Oh, H. Y.; Lee, C.; Lee, S. *Org. Electron.* **2009**, *10*, 163−169. (e) Gu, J.-F.; Xie, G.-H.; Zhang, L.; Chen, S.-F.; Lin, Z.-Q.; Zhang, Z.-S.; Zhao, J.-F.; Xie, L.-H.; Tang, C.; Zhao, Y.; Liu, S.-Y.; Huang, W. *J. Phys. Chem. Lett.* **2010**, *1*, 2849−2853. (f) Figueira-Duarte, T. M.; Müllen, K. *Chem. Rev.* **2011**, *111*, 7260−7314.

(10) (a) Li, S.; Jia, Z. Y.; Nakajima, K.; Kanno, K.; Takahashi, T. *J. Org. Chem.* **2011**, *76*, 9983−9987. (b) Lei, T.; Zhou, Y.; Cheng, C. Y.; Cao, Y.; Peng, Y.; Bian, J.; Pei, J. *Org. Lett.* **2011**, *13*, 2642−2645. (c) Katsuta, S.; Miyagi, D.; Yamada, H.; Okujima, T.; Mori, S.; Nakayama, K.; Uno, H. *Org. Lett.* **2011**, *13*, 1454−1457. (d) Qu, H. M.; Cui, W. B.; Li, J. L.; Shao, J. J.; Chi, C. Y. *Org. Lett.* **2011**, *13*, 924−927.

(11) (a) Ren, M.-G.; Guo, H.-J.; Qi, F.; Song, Q.-H. *Org. Biomol. Chem.* **2011**, *9*, 6913−6916. (b) Chen, Y.-M.; Hung, W.-Y.; You, H.-W.; Chaskar, A.; Ting, H.-C.; Chen, H.-F.; Wong, K.-T.; Liu, Y.-H. *J. Mater. Chem.* **2011**, *21*, 14971−14978. (c) Hoffmann, S. T.; Schrogel, P.; Rothmann, M.; Albuquerque, R. Q.; Strohriegl, P.; Kohler, A. *J. Phys. Chem. B* **2011**, *115*, 414−421. (d) Salman, S.; Kim, D.; Coropceanu, V.; Bredas, J. L. *Chem. Mater.* **2011**, *23*, 5223−5230. (e) Pandya, S. U.; Al Attar, H. A.; Jankus, V.; Zheng, Y. H.; Bryce, M. R.; Monkman, A. P. *J. Mater. Chem.* **2011**, *21*, 18439−18446. (f) Gong, S.; He, X.; Chen, Y.; Jiang, Z.; Zhong, C.; Ma, D.; Qin, J.; Yang, C. *J. Mater. Chem.* **2012**, *22*, 2894−2899.

(12) Kozma., E.; Munno, F.; Kotowski, D.; Bertini, F.; Luzzati, S.; Catellani, M. *Synth. Met.* **2010**, *160*, 996−1001.

(13) (a) Zang, L.; Che, Y.; Moore, J. S. *Acc. Chem. Res.* **2008**, *41*, 1596−1608. (b) Teng, C.; Yang, X. C.; Yang, C.; Li, S. F.; Cheng, M.; Hagfeldt, A.; Sun, L. C. *J. Phys. Chem. C* **2010**, *114*, 9101−9110.

(14) (a) Kale, T. S.; Krishnamoorthy, K.; Thelakkat, M.; Thayumanavan, S. *J. Phys. Chem. Lett.* **2010**, *1*, 1116−1121. (b) Xiao, J.; Xu, J.; Cui, S.; Liu, H.; Wang, S.; Li, Y. *Org. Lett.* **2008**,

10, 645−648. (c) Hancock, J. M.; Gifford, A. P.; Tonzola, C. J.; Jenekhe, S. A. *J. Phys. Chem. C* **2007**, *111*, 6875−6882. (d) Bernhardt, S.; Kastler, M.; Enkelmann, V.; Baumgarten, M.; Müllen, K. *Chem.—Eur. J.* **2006**, *12*, 6117−6128.
(15) (a) Wong, K.-T.; Chien, Y.-Y.; Chen, R.-T.; Wang, C.-F.; Lin, Y.-T.; Chiang, H.-H.; Hsieh, P.-Y.; Wu, C.-C.; Chou, C. H.; Su, Y. O.; Lee, G.-H.; Peng, S.-M. *J. Am. Chem. Soc.* **2002**, *124*, 11576−11577. (b) Setayesh, S; Grimsdale, A. C.; Weil, T.; Enkelmann, V.; Müllen, K.; Meghdadi, F.; List, E. J. W.; Leising, G. *J. Am. Chem. Soc.* **2001**, *123*, 946−953.
(16) (a) Tang, C.; Liu, F.; Xia, Y.-J.; Lin, J.; Xie, L.-H.; Zhong, G.-Y.; Fan, Q.-L.; Huang, W. *Org. Electron.* **2006**, *7*, 155−162. (b) Tang, C.; Liu, F.; Xia, Y.-J.; Xie, L.-H.; Wei, A.; Li, S.-B.; Fan, Q.-L.; Huang, W. *J. Mater. Chem.* **2006**, *16*, 4074−4080. (c) Liu, F.; Xie, L.-H.; Tang, C.; Liang, J.; Chen, Q.-Q.; Peng, B.; Wei, W.; Cao, Y.; Huang, W. *Org. Lett.* **2009**, *11*, 3850−3853.
(17) (a) Zhao, Z.; Xu, X.; Jiang, Z.; Lu, P.; Yu, G.; Liu, Y. *J. Org. Chem.* **2007**, *72*, 8345−8353. (b) Zhao, Z.; Xu, X.; Wang, H.; Lu, P.; Yu, G.; Liu, Y. *J. Org. Chem.* **2008**, *73*, 594−602. (c) Zhao, Z.; Li, J.-H.; Chen, X.; Wang, X.; Lu, P.; Yang, Y. *J. Org. Chem.* **2009**, *74*, 383−395.
(18) (a) Halleux, V.; Calbert, J.-P.; Brocorens, P.; Cornil, J.; Declercq, J.-P.; Brédas, J. -L.; Geerts, Y. *Adv. Funct. Mater.* **2004**, *14*, 649−659. (b) Zhang, H.; Wang, Y.; Shao, K.; Liu, Y.; Chen, S.; Qiu, W.; Sun, X.; Qi, T.; Ma, Y.; Yu, G.; Su, Z.; Zhu, D. *Chem. Commun.* **2006**, 755−757.
(19) (a) Moorthy, J. N.; Natarajan, P.; Venkatakrishnan, P.; Huang, D.-F.; Chow, T. J. *Org. Lett.* **2007**, *9*, 5215−5218. (b) Sonar, P.; Soh, M. S.; Cheng, Y. H.; Henssler, J. T.; Sellinger, A. *Org. Lett.* **2010**, *12*, 3292−3295. (c) Hu, J. -Y.; Era, M.; Elsegood, M. R. J.; Yamato, T. *Eur. J. Org. Chem.* **2010**, 72−79. (d) Kim, H. M.; Lee, Y. O.; Lim, C. S.; Kim, J. S.; Cho, B. R. *J. Org. Chem.* **2008**, *73*, 5127−5130. (e) Sung, J.; Kim, P.; Lee, Y. O.; Kim, J. S.; Kim, D. *J. Phys. Chem. Lett.* **2011**, *2*, 818−823.
(20) Kang, H.; Evmenenko, G.; Dutta, P.; Clays, K.; Song, K.; Marks, T. J. *J. Am. Chem. Soc.* **2006**, *128*, 6194−6205.
(21) Wilson, J. N.; Josowicz, M.; Wang, Y.; Bunz, U. H. F. *Chem. Commun.* **2003**, 2962−2963.
(22) Samori, S.; Tojo, S.; Fujitsuka, M.; Spilter, E. L.; Haley, M. M.; Majima, T. *J. Org. Chem.* **2008**, *73*, 3551−3558.
(23) Cai, L.; Zhan, R.; Pu, K.-Y.; Qi, X.; Zhang, H.; Huang, W.; Liu, B. *Anal. Chem.* **2011**, *83*, 7849−7855.
(24) Wan, Y.; Yan, L.; Zhao, Z.; Ma, X.; Guo, Q.; Jia, M.; Lu, P.; Ramos-Ortiz, G.; Maldonado, J. L.; Rodríguez, M.; Xia, A. *J. Phys. Chem. B* **2010**, *114*, 11737−11745.
(25) (a) Sorensen, J. K.; Fock, J.; Pedersen, A. H.; Petersen, A. B.; Jennum, K.; Bechgaard, K.; Kilsa, K.; Geskin, V.; Cornil, J.; Bjornholm, T.; Nielsen, M. B. *J. Org. Chem.* **2011**, *76*, 245−263.
(26) Jones, G.; Jackson, W. R.; Choi, C.; Bergmark, W. R. *J. Phys. Chem.* **1985**, *89*, 294−300.
(27) Crawford, A. G.; Dwyer, A. D.; Liu, Z.; Steffen, A.; Beeby, A.; Pålsson, L.-O.; Tozer, D. J.; Marder, T. B. *J. Am. Chem. Soc.* **2011**, *133*, 13349−13362.
(28) Yang, S.-W.; Elangovan, A.; Hwang, K.-C; Ho, T.-I. *J. Phys. Chem. B* **2005**, *109*, 16628−16635.
(29) Venkataramana, G.; Sankararaman, S. *Org. Lett.* **2006**, *8*, 2739−2742.
(30) Liu, F.; Lai, W.-Y.; Tang, C.; Wu, H.-B.; Chen, Q.-Q.; Peng, B.; Wei, W.; Huang, W.; Cao, Y. *Macromol. Rapid Commun.* **2008**, *29*, 659−664.
(31) (a) Nantalaksakul, A.; Mueller, A.; Klaikherd, A.; Bardeen, C. J.; Thayumanavan, S. *J. Am. Chem. Soc.* **2009**, *131*, 2727−2738. (b) Thomas, K. R. J.; Thompson, A. L.; Sivakumar, A. V.; Bardeen, C. J.; Thayumanavan, S. *J. Am. Chem. Soc.* **2005**, *127*, 373−383. (c) Thomas, K. R. J.; Kapoor, N.; Lee, C.-P.; Ho, K.-C. *Chem.—Asian J.* **2012**, *7*, 738−750.
(32) Kapoor, N.; Thomas, K. R. J. *New J. Chem.* **2010**, *34*, 2739−2748.
(33) (a) Lippert, E. *Z. Naturforsch.* **1955**, *10A*, 541−545. (b) Mataga, N.; Kaifu, Y.; Koizumi, M. *Bull. Chem. Soc. Jpn.* **1956**, *29*, 465−470.
(34) (a) Granzhan, A.; Ihmels, H.; Viola, G. *J. Am. Chem. Soc.* **2007**, *129*, 1254−1267. (b) van den Berg, O.; Jager, W. F.; Picken, S. J. *J. Org. Chem.* **2006**, *71*, 2666−2676.
(35) Sherwood, G. A.; Cheng, R.; smith, T. M.; Werner, J. H.; Shreve, A. P.; Peteanu, L. A.; Wildeman, J. *J. Phys. Chem. C* **2009**, *113*, 18851−18862.
(36) Ego, C.; Grimsdale, A. C.; Uckert, F.; Yu, G.; Srdanov, G.; Müllen, K. *Adv. Mater.* **2002**, *14*, 809−811.
(37) Parr, R. G.; Yang, W. T. *Annu. Rev. Phys. Chem.* **1995**, *46*, 701−728.
(38) Lynch, B. J.; Fast, P. L.; Harris, M.; Truhlar, D. G. *J. Phys. Chem. A* **2000**, *104*, 4811−4815.
(39) Ji, S.; Yang, J.; Yang, Q.; Liu, S.; Chen, M.; Zhao, J. *J. Org. Chem.* **2009**, *74*, 4855−4865.
(40) Li, Z. H.; Wong, M. S.; Tao, Y.; Lu, J. *Chem.—Eur. J.* **2005**, *11*, 3285.
(41) Frisch, M. J.; Trucks, G. W.; Schlegel, H. B.; Scuseria, G. E.; Robb, M. A.; Cheeseman, J. R.; Scalmani, G.; Barone, V.; Mennucci, B.; Petersson, G. A.; Nakatsuji, H.; Caricato, M.; Li, X.; Hratchian, H. P.; Izmaylov, A. F.; Bloino, J.; Zheng, G.; Sonnenberg, J. L.; Hada, M.; Ehara, M.; Toyota, K.; Fukuda, R.; Hasegawa, J.; Ishida, M.; Nakajima, T.; Honda, Y.; Kitao, O.; Nakai, H.; Vreven, T.; Montgomery, J. A., Jr.; Peralta, J. E.; Ogliaro, F.; Bearpark, M.; Heyd, J. J.; Brothers, E.; Kudin, K. N.; Staroverov, V. N.; Kobayashi, R.; Normand, J.; Raghavachari, K.; Rendell, A.; Burant, J. C.; Iyengar, S. S.; Tomasi, J.; Cossi, M.; Rega, N.; Millam, N. J.; Klene, M.; Knox, J. E.; Cross, J. B.; Bakken, V.; Adamo, C.; Jaramillo, J.; Gomperts, R.; Stratmann, R. E.; Yazyev, O.; Austin, A. J.; Cammi, R.; Pomelli, C.; Ochterski, J. W.; Martin, R. L.; Morokuma, K.; Zakrzewski, V. G.; Voth, G. A.; Salvador, P.; Dannenberg, J. J.; Dapprich, S.; Daniels, A. D.; Farkas, Ö .; Foresman, J. B.; Ortiz, J. V.; Cioslowski, J.; Fox, D. J. *Gaussian 09*, revision A.02; Gaussian, Inc.: Wallingford, CT, 2009.
(42) (a) Lee, C.; Yang, W.; Parr, R. G. *Phys. Rev. B* **1988**, *37*, 785−789. (b) Becke, A. D. *J. Chem. Phys.* **1993**, *98*, 1372−1377.